LLNL-TR-729937

Lawrence Livermore National Laboratory

Magnetotelluric Detection Thresholds as a Function of Leakage Plume Depth, TDS and Volume

Xianjin Yang, Thomas A. Buscheck, Kayyum Mansoor, Susan A. Carroll

April 21, 2017

This technical report is a deliverable at a milestone M1.17.4.B for US DOE National Risk Assessment Partnership (NRAP Phase II) Strategic Monitoring Subtask 4.1: Development of Methods to Model Monitoring Techniques. NRAP is funded through the DOE Office of Fossil Energy and National Energy Technology Laboratory.

Disclaimer

Lawrence Livermore National Laboratory is operated by Lawrence Livermore National Security, LLC, for the U.S. Department of Energy, National Nuclear Security Administration under Contract DE-AC52-07NA27344.

Table of Contents

Abstract

We conducted a synthetic magnetotelluric (MT) data analysis to establish a set of specific thresholds of plume depth, TDS concentration and volume for detection of brine and CO_2 leakage from legacy wells into shallow aquifers in support of Strategic Monitoring Subtask 4.1 of the US DOE National Risk Assessment Partnership (NRAP Phase II), which is to develop geophysical forward modeling tools. 900 synthetic MT data sets span 9 plume depths, 10 TDS concentrations and 10 plume volumes. The monitoring protocol consisted of 10 MT stations in a 2×5 grid laid out along the flow direction. We model the MT response in the audio frequency range of 1 Hz to 10 kHz with a 50 Ω·m baseline resistivity and the maximum depth up to 2000 m. Scatter plots show the MT detection thresholds for a trio of plume depth, TDS concentration and volume. Plumes with a large volume and high TDS located at a shallow depth produce a strong MT signal. We demonstrate that the MT method with surface based sensors can detect a brine and CO_2 plume so long as the plume depth, TDS concentration and volume are above the thresholds. However, it is unlikely to detect a plume at a depth larger than 1000 m with the change of TDS concentration smaller than 10%. Simulated aquifer impact data based on the Kimberlina site provides a more realistic view of the leakage plume distribution than rectangular synthetic plumes in this sensitivity study, and it will be used to estimate MT responses over simulated brine and CO_2 plumes and to evaluate the leakage detectability. Integration of the simulated aquifer impact data and the MT method into the NRAP DREAM tool may provide an optimized MT survey configuration for MT data collection. This study presents a viable approach for sensitivity study of geophysical monitoring methods for leakage detection. The results come in handy for rapid assessment of leakage detectability.

1 Introduction

Geologic carbon sequestration (GCS) is considered to be an effective approach to mitigate rising carbon dioxide (CO_2) concentrations in the atmosphere. CO_2 stored in a deep geologic reservoir may leak into overlying aquifers through degraded and abandoned wells and subsequently dissolve in aquifers degrading water quality. Pressurized brine with high total dissolved solids (TDS) may also be driven up a leaky wellbore. Combined CO_2 and brine leakage will contaminate underground sources of drinking water (USDW) by lowering the pH and increasing TDS content of the groundwater. Brine and CO_2 leakage in shallow aquifers can be detected by geochemical sampling [*Cahill and Jakobsen*, 2013; *Carroll et al.*, 2009; *Kharaka et al.*, 2010], pressure monitoring [*Nogues et al.*, 2011; *W Trainor-Guitton et al.*, 2016] and electrical geophysical imaging methods such as electrical resistivity tomography [*Yang et al.*, 2015] and controlled source electromagnetic (EM) imaging [*Girard et al.*, 2011]. However, geochemical and pressure monitoring methods provide in-situ point measurements only. These monitoring methods all require deployment of sensors in expensive monitoring wells, which may introduce new leakage pathways.

The magnetotelluric (MT) method is a surface based geophysical imaging technique which has been deployed to monitor CO_2 storage at the Hontomin CO_2 storage site in Spain [*Ogaya Garcia*, 2014; *Ogaya et al.*, 2013; *Ogaya et al.*, 2014]. Synthetic data suggests that a minimum 1.8 megaton supercritical CO_2 at 1500 m depth is needed to produce an observable MT anomaly on the surface. No publication has been found on monitoring dissolved CO_2 in groundwater aquifers using the MT method.

In this study, we assess the detectability of wellbore brine and CO_2 leakage using the MT forward modeling method and synthetic leakage plume models in support of Strategic Monitoring Subtask 4.1 of the US DOE National Risk Assessment Partnership (NRAP Phase II) to develop geophysical forward modeling tools with necessary physics. Our synthetic study is based on the Kimberlina site in the southern San Joaquin Basin, California. The aquifer depth is as large as 1700m. The MT method can detect plumes at depths of thousands of meters without any costly monitoring wells. Abandoned wells can be located effectively by airborne magnetic methods [*Hammack et al.*, 2006] and multiple MT monitoring stations can be deployed around an abandoned well for detection of CO_2 and brine leakage in a large area.

2 Magnetotelluric Method

The magnetotelluric (MT) method is a surface geophysical technique that uses the earth's natural electric and magnetic fields to probe the electrical resistivity structure of the earth from tens of meters to hundreds of kilometers [*Chave and Jones*, 2012; *Simpson and Bahr*, 2005]. Electrical

resistivity of a rock is a complex function of porosity, pore fluid salinity and saturation, temperature and clay contents. The typical resistivity values of common rock types are shown in Figure 1 [*Palacky*, 1988]. Variations of water salinity and grain size result in many orders of magnitude changes of medium resistivity. The widely used Archie's equation [*Archie*, 1942] describes between resistivity of the clay free sandstone and porosity, fluid resistivity and saturation.

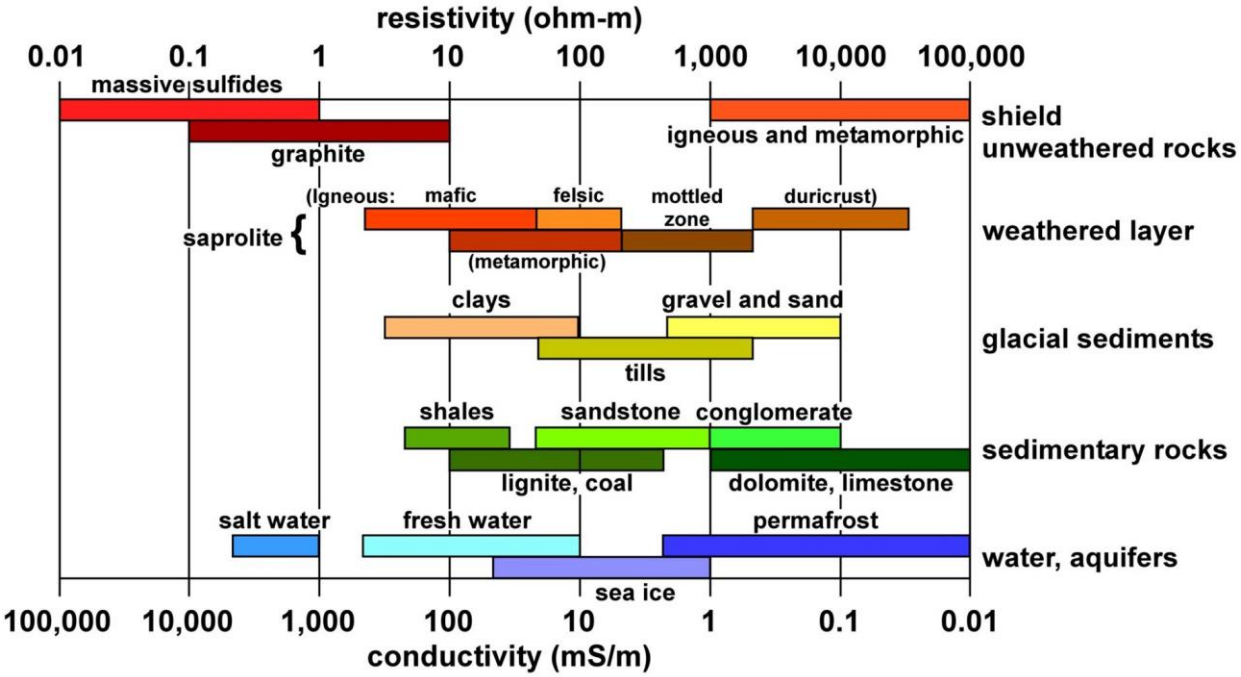

Figure 1. Typical resistivity values of common earth materials [*Palacky*, 1988].

Brine and CO_2 leakage in groundwater aquifers increases ion concentrations, which results in elevated water electrical conductivity (EC). The ion properties and concentrations are used to estimate water EC by Eq. (1) below.

$$EC = \sum_{s=1}^{n} |z_s| \lambda_s c_s \qquad (1),$$

where c_s is ion concentration, z_s is number of electrons per ion and λ_s is ionic conductivity. Four common species in a leakage scenario are Na^+, Cl^-, Ca^{2+} and HCO_3^-.

The MT method is a passive geophysical imaging method without an active transmitter. The natural electromagnetic source fields consist of (1) micro-pulsations (< 1Hz) due to the interaction of solar wind with the geomagnetic field; and (2) global lightning activities (> 1Hz). The energy generated by lightning travels around the earth in a waveguide between the earth

surface and the ionosphere. The large-scale passive electromagnetic source fields are treated as uniform plane waves propagating vertically into the earth.

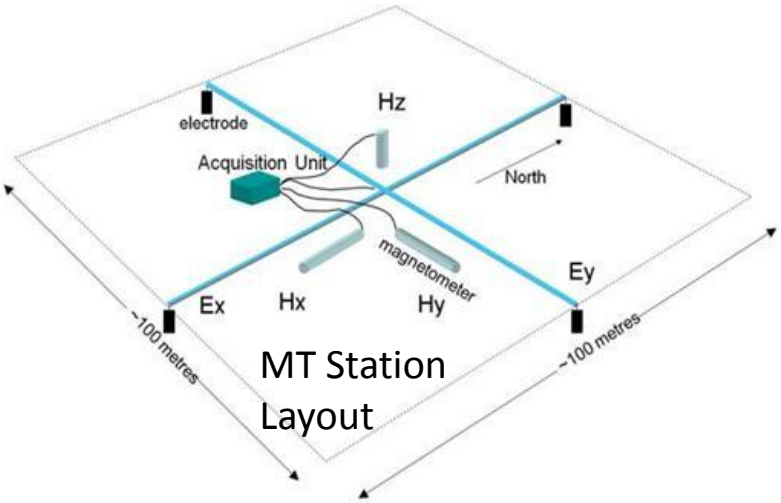

http://en.openei.org/wiki/Magnetotellurics

http://www.kmstechnologies.com/MT_survey_system.html

Figure 2. The field setup of an MT station with two electric field dipoles (Ex and Ey) and three orthogonal magnetic coils (Hx, Hy and Hz). The lower image shows MT equipment with magnetometer coils (black long cylinders) and four electrodes (gray and yellow).

Two electric field components (Ex and Ey) and three magnetic field components (Hx, Hy and Hz) are measured at a station (Figure 2). Time series of natural electric and magnetic fields are recorded simultaneously at each MT station and are transformed into the impedance tensor in frequency domain.

The MT method is a frequency sounding technique. An EM signal at a lower frequency penetrates deeper. The depth of penetration (d in meters), the MT skin depth, can be estimated from the EM signal frequency (f in Hz) and material resistivity (ρ in Ω·m) by:

$$d = 503\sqrt{\rho/f} \qquad (2)$$

For a medium of 100 Ω·m, the MT signal with the lowest possible frequency of 0.0001 Hz can penetrate hundreds of kilometers. At the highest frequency of 10 kHz, the penetration depth is around 50 m. The MT method does not have adequate resolution from the surface to 100 m depth.

3 Synthetic Magnetotelluric Data

As mentioned in the Introduction, leakage of CO_2 and brine into groundwater changes the pore species concentrations (Na+, Cl-, HCO_3-, H+, Ca2+, CO_2 (gas) and CO_2 (aqueous)) and electrical conductivity (EC). The pore fluid EC can be estimated directly from these ion concentrations [Visconti et al., 2010]. The bulk formation EC is obtained through Archie's equation [Archie, 1942] with knowledge of the formation porosity and water saturation. This sensitivity study generates synthetic MT data without prior reservoir and flow models. We used synthetic data to assess the thresholds for detecting brine and CO_2 leakage using the MT method.

The synthetic electrical conductivity model is roughly based on the Kimberlina site, located in the southern portion of California's San Joaquin Valley. The pre-injection baseline model is assumed to be a homogeneous half space with a constant porosity of 0.30 and constant water TDS concentration of 2000 mg/L. The bulk resistivity of the formation is estimated at about 50 Ω·m [Archie, 1942; Reluy et al., 2004].

The MT signal frequency range can be determined using the skin depth Eq. (2) with the known formation resistivity. We set the higher frequency at 10 kHz that gives a skin depth of 35 m to resolve changes at a shallow depth of 50 m. The lower frequency depends on the depth of investigation, which is about 1700 m for the Kimberlina site. The skin depth for the 1 Hz MT signal is about 3500 m, which meets the requirement of penetration depth. From 1 Hz to 10 kHz, we chose 17 logarithmically-spaced frequencies with 4 frequency points per decade. The MT method in this frequency range is often referred to as audio-frequency MT or AMT.

The MT signal strength depends on the number of brine and CO_2 plumes, and the size, shape, species concentration and depth of an individual plume. We ignore the effect of resistive gaseous and supercritical CO_2, and simulate one electrically conductive plume with elevated species concentration due to brine leakage and CO_2 dissolution in groundwater. The MT method is sensitive to the relative change of electrical conductivity that is linearly dependent on the fluid TDS. We study the MT detection thresholds by running MT forward models with combinations of 9 plume depths, 10 volumes and 10 TDS concentrations (Table 1) for a total of 900 MT synthetic datasets. The maximum plume depth is determined based on the maximum aquifer depth of 1700 m at the Kimberlina site. The maximum TDS increase in a shallow aquifer due to

CO_2 leakage can exceed 200% [*W J Trainor-Guitton et al.*, 2013]. The synthetic plume is symmetric to the leaky wellbore and it expands in three dimensions with greatest growth along the groundwater flow direction (Figure 2).

Table 1. MT simulation parameters for 900 MT synthetic datasets

No.	Depth (m)	TDS Increase (%)	Volume (m^3 = L×W×H)
1	50	0	1×10^6 = 100×100×100
2	100	10	2×10^6 = 200×100×100
3	200	25	4×10^6 = 200×200×100
4	400	50	8×10^6 = 400×200×100
5	600	75	1.6×10^7 = 400×200×200
6	800	100	3.2×10^7 = 800×200×200
7	1000	125	6.4×10^7 = 800×400×200
8	1200	150	1.28×10^8 = 1600×400×200
9	1400	175	2.56×10^8 = 1600×800×200
10		200	5.12×10^8 = 1600×800×400

MT forward simulations were conducted at 10 stations in a grid of 2 lines by 5 stations per line (Figure 1). The station spacing is 200 m and the line separation is 400 m. This MT station configuration provides information for optimization of MT survey design. The CO_2 plume starts from the leaky wellbore and grows mainly along the direction of the regional groundwater flow (Figure 2).

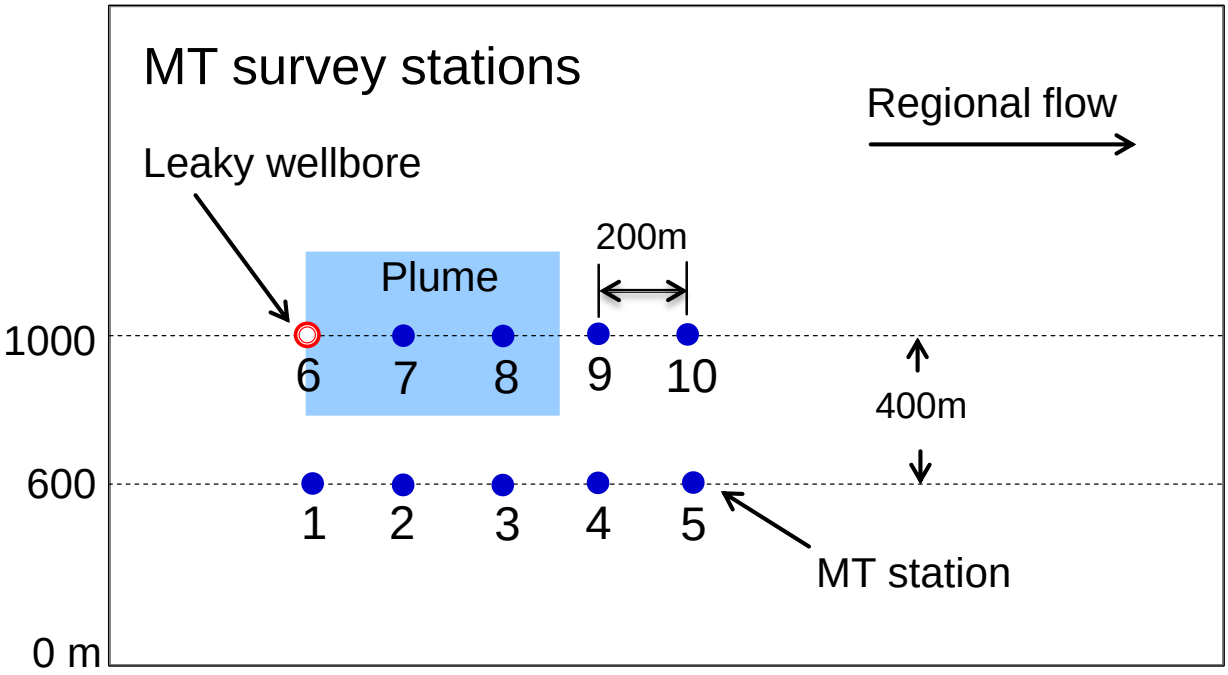

Figure 1. Locations of 10 MT survey stations and one leaky wellbore.

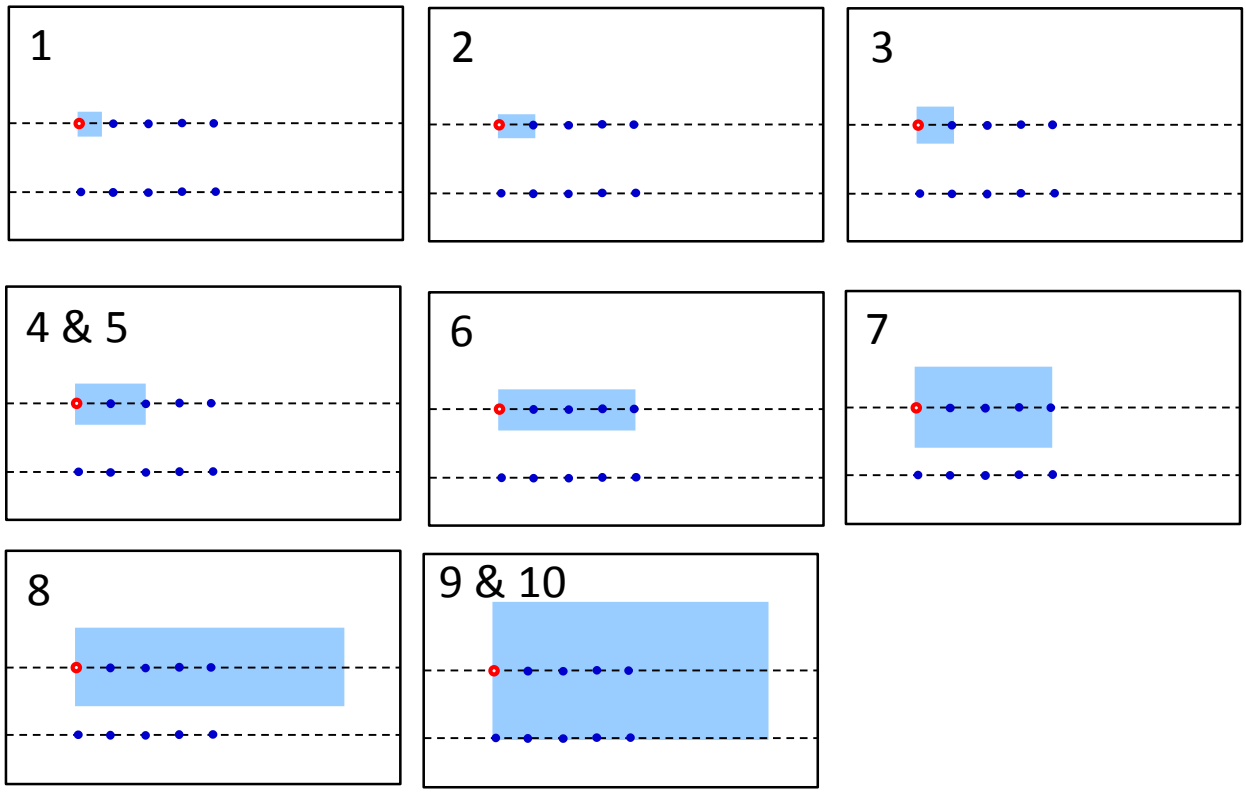

Figure 2. Plan view of the plume locations relative to the leaky wellbore and MT stations.

ModEM, a 3D MT forward model and inversion software, was used to generate synthetic MT data [*Kelbert et al.*, 2014]. In this study ModEM takes inputs of station locations, signal frequencies, an electrical resistivity model and 3D modeling mesh and predicts the MT impedance tensor (Z_{xx}, Z_{xy}, Z_{yx}, Z_{yy}) shown in Eq. (3).

$$\begin{pmatrix} E_x \\ E_y \end{pmatrix} = \begin{pmatrix} Z_{xx} & Z_{xy} \\ Z_{yx} & Z_{yy} \end{pmatrix} \begin{pmatrix} H_x \\ H_y \end{pmatrix} \qquad (3)$$

The electromagnetic fields are often decoupled into two independent modes. One mode has the electric field parallel to the strike of a structure, i.e., E-polarization or transverse electric (TE) mode, and another mode has the magnetic field parallel to the strike, i.e., B-polarization or transverse magnetic (TM) mode. The complex impedance tensor is then used to estimate the more intuitive apparent resistivity and phase in TE and TM modes for ease of data visualization. In the TE mode, the apparent resistivity (ρ_{xy}) and phase (φ_{xy}) are given by

$$\rho_{xy}(\omega) = \frac{1}{\mu_0 \omega} \left| Z_{xy}(\omega) \right|^2 \qquad (4)$$

$$\varphi_{xy}(\omega) = \tan^{-1}\left(\frac{\mathrm{Im}\{Z_{xy}\}}{\mathrm{Re}\{Z_{xy}\}}\right) \quad (5)$$

The magnetic permeability in free space (μ_0) is a constant, $\mu 0 = 4\pi\times10^{-7}$ H/m. It is used to approximate the magnetic permeability of the earth. In the TM mode, we have

$$\rho_{yx}(\omega) = \frac{1}{\mu_0\omega}\left|Z_{yx}(\omega)\right|^2 \quad (6)$$

$$\varphi_{yx}(\omega) = \tan^{-1}\left(\frac{\mathrm{Im}\{Z_{yx}\}}{\mathrm{Re}\{Z_{yx}\}}\right) \quad (7)$$

Both apparent resistivity and phase are a function of angular frequency (ω). For a uniform half space, the apparent resistivity in both TE and TM modes is equal to the true resistivity of the earth, and the phase will be 45°, indicating that the electric field precedes the magnetic field by 45°. These diagnostic measures are a good indicator of MT forward model accuracy.

4 Results

900 MT synthetic data sets are generated by sampling three parameters: plume depth, TDS concentration and plume volume. For each data set, MT data are available at 10 stations. We chose a few plots of apparent resistivity and phase in the TE mode to show the MT sensitivity to changes of these parameters. Figure 3 shows that the apparent resistivity (ρ_{xy}) is sensitive to changes in plume depth, TDS increase and volume. Note that the baseline apparent resistivity without a plume is 50 Ω·m. The conductive plume with elevated TDS lowers the apparent resistivity. The maximum reduction in apparent resistivity is 25 Ω·m or 50%. The baseline phase without a plume is 45°. A conductive plume increases the phase. The maximum phase increase is > 6° or > 13%. Figure 4 shows the sensitivity of the phase to the changes of plume depth, TDS concentration and plume volume. The plume depth, sampled linearly, seems the most sensitive parameter. The baseline phase without a plume is 45°. A conductive plume increases the phase. The maximum phase increase is > 6° or >13%.

We define that the detection of a leak is to observe > 5% change in either apparent resistivity or phase compared with the baseline data in any of 17 frequencies in the synthetic data. By analyzing all 900 synthetic datasets, we find the detection thresholds at various plume depth, TDS and volume (Fig. 5). A plume with 100% TDS increase at 50 m depth must have a volume of 2×10^6 m^3 (0.02 km^2 x 100-m thick plume) to be detectable (refer to the label (1) in Fig. 5). It is clear that a plume with a larger TDS and at a shallower depth can be detected with a much smaller volume. Detection of a plume below 1000 m depth requires an unrealistically large

plume volume and change in TDS concentration. It is unlikely that a plume below 1000 m depth will be detectable.

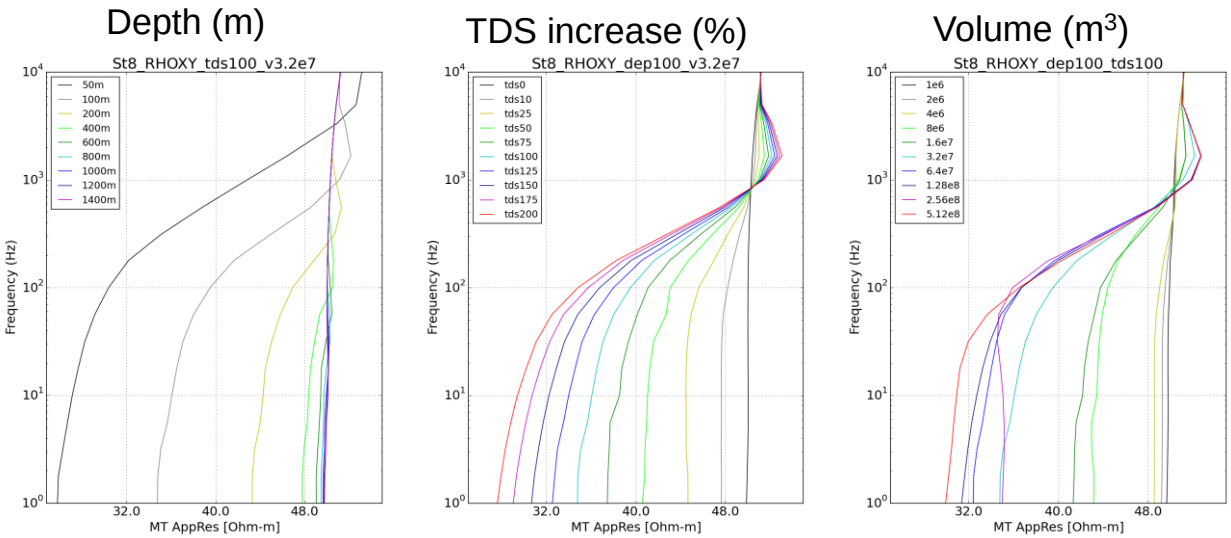

Figure 3. Sensitivity of the apparent resistivity to plume depth, TDS increase and volume at the MT station 8.

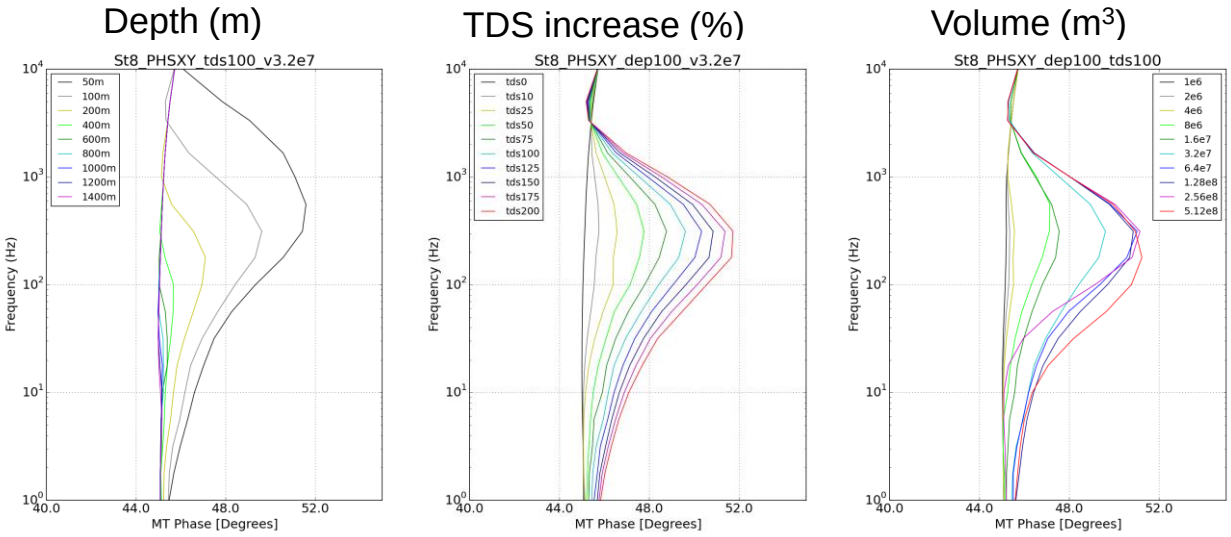

Figure 4. Sensitivity of the phase to plume depth, TDS increase and volume at the MT station 8.

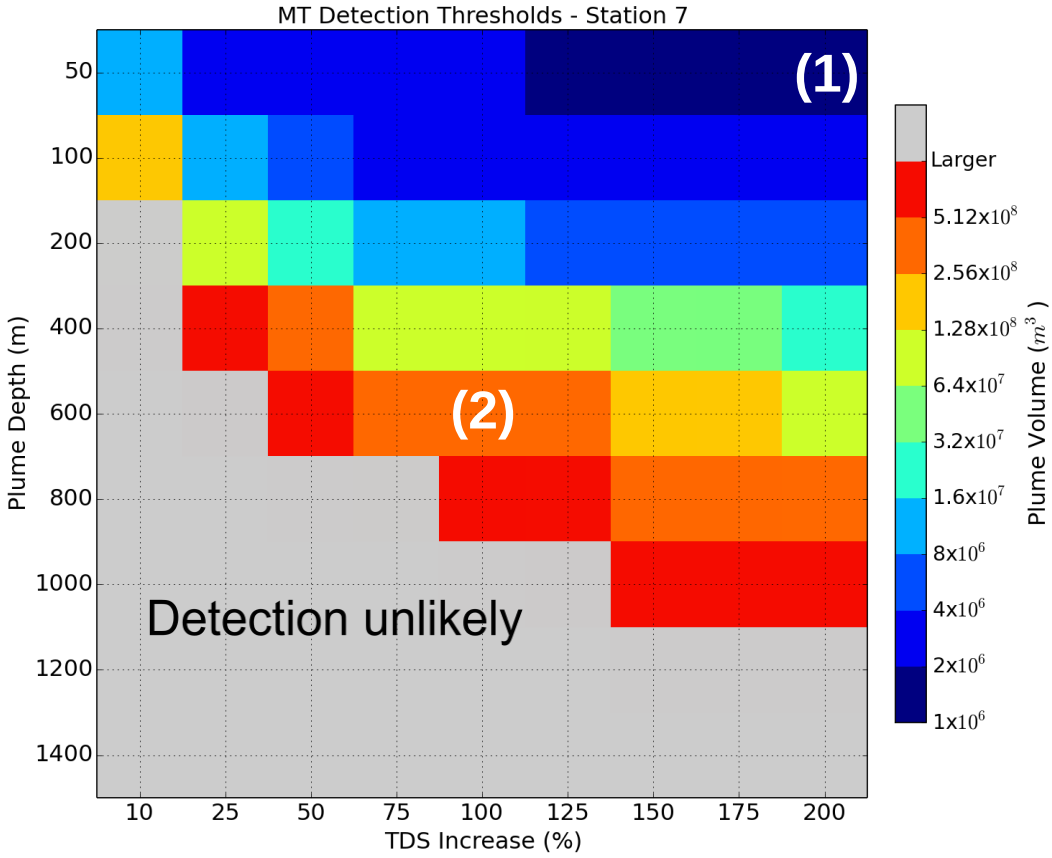

Figure 5. Detection thresholds at various plume depth, TDS and volume at the MT station 7.

The detection threshold not only depends on the plume depth, TDS and volume, but also on the MT sensor location (Fig. 6). MT can detect a plume of smaller volume when the sensor is directly on top of the plume, such as Stations 6, 7, and 8. Although MT can detect a plume not directly below a sensor, it requires a much larger plume.

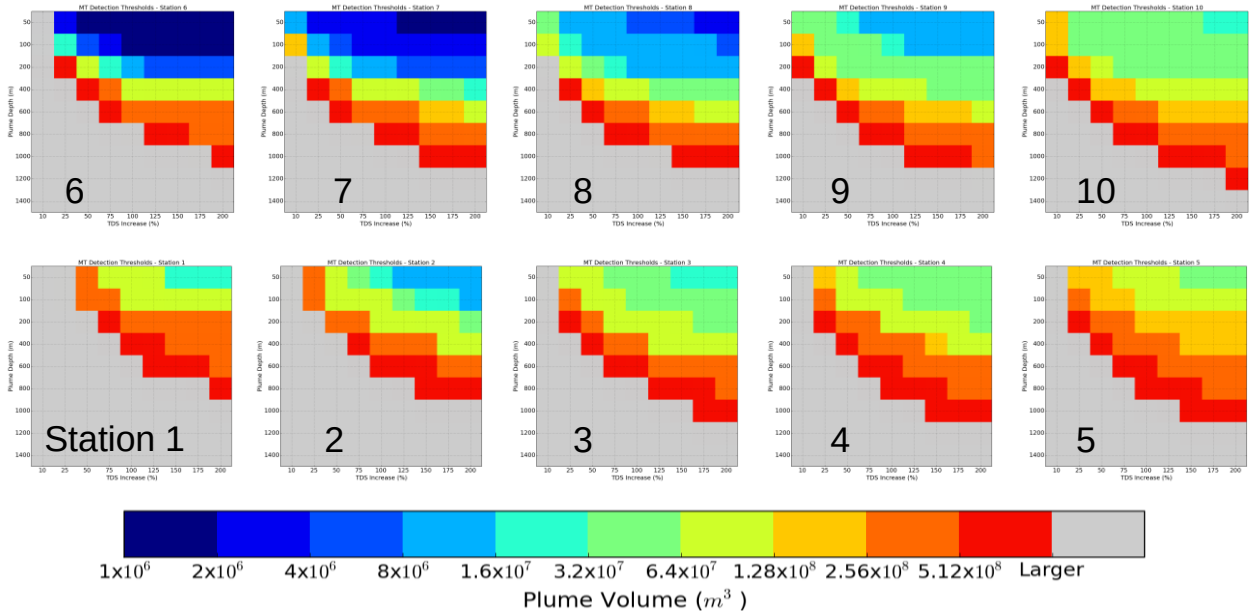

Figure 6. Detection thresholds at 10 MT stations (refer to Fig. 1 for MT sensor locations).

5 Discussion and Conclusion

This study is based on noise free synthetic MT data with a homogeneous baseline conductivity model. The field MT surveys are sensitive to environmental noise such as well casing, pipelines and powerlines. We used a noise level of 5% to distinguish between noise and a reliable MT signal. This approach is supported by other studies. The MT experimental error of 10% for apparent resistivity and 2.9° for the phase are mentioned in the Hontomin MT work [Ogaya Garcia, 2014], who implied that a layer stripping method can reduce the noise level to 2-3%.

The audio frequency magnetotellurics (AMT) method in this study provides MT responses in the frequency range of 1 Hz – 10 kHz and it is suitable for shallow investigation from 50 m to 2 km depth. The advantage of AMT is that it includes fast data collection and a large number of data stacks for noise reduction. The disadvantage is that AMT dead bands around 1 Hz and from 1 kHz to 5 kHz have an unstable energy source with diurnal and annual variation [Garcia and Jones, 2008; García and Jones, 2005; Iliceto and Santarato, 1999] and they compromise AMT data quality. To overcome this deficiency, researchers developed effective data acquisition and processing methods [*Garcia and Jones*, 2008; *García and Jones*, 2005]. An alternative approach to improve the signal to noise ratio is to use the controlled source audio frequency magnetotellurics method with an active source [*Streich et al.*, 2010].

A disadvantage of the MT method is its inability to detect subsurface changes in a shallow depth from 0 m to 50 m. The electrical resistivity tomography (ERT) method is sensitive to the near surface zone and may provide complementary information at the shallow depth.

Our synthetic MT data analysis provides a set of thresholds of plume depth, TDS concentration and volume as a guideline for detection of brine and CO_2 leakage in shallow aquifers using MT surveys. It is clear that the MT signal strength depends on the plume depth, TDS, volume and the relative location between the sensor and plume center. A plume with a large volume and high TDS and at a shallow depth produces a strong MT signal. An MT sensor directly above the center of a plume is an ideal location for plume detection. We demonstrate that the MT method with surface based sensors can detect a brine and CO_2 plume as long as the plume depth, TDS concentration and volume are above the thresholds. A grid of MT survey stations can monitor a large area and improve the detectability. However, it is unlikely to detect a plume at a depth larger than 1000 m and with the change of TDS concentration smaller than 10%.

The rectangular shape of synthetic plumes in this study is used for convenience of MT model building. Simulated plumes by multi-phase flow and reactive transport models are more realistic. Simulated aquifer impact data based on the Kimberlina site [Buscheck et al., 2017] will be used to estimate MT responses over simulated brine and CO_2 plumes and evaluate the leakage detectability. Integration of the simulated aquifer impact data and MT method into the NRAP DREAM tool may provide an optimized MT survey configuration with optimal number of stations, station spacing and timing for MT data collection.

This work presents a viable approach for sensitivity study of geophysical monitoring methods for leakage detection. The results come in handy for rapid assessment of leakage detectability.

Reference

Archie, G. E. (1942), The electrical resistivity log as an aid in determining some reservoir characteristics, *T Am I Min Met Eng*, *146*, 54-61.

Buscheck, T.A., Mansoor, K., Yang, X., and Carroll, S.A. (2017), Simulated Aquifer Impact Data for Testing Wellbore Leakage Monitoring Techniques, Rev. 1.1, Technical Report for National Risk Assessment Partnership (NRAP) Subtask 4.1: Development of Methods to Model Monitoring Techniques, LLNL-TR-731055, Lawrence Livermore National Laboratory, Livermore, CA, USA.

Cahill, A. G., and R. Jakobsen (2013), Hydro-geochemical impact of CO_2 leakage from geological storage on shallow potable aquifers: A field scale pilot experiment, *Int J Greenh Gas Con*, *19*, 678-688.

Carroll, S., Y. Hao, and R. Aines (2009), Geochemical detection of carbon dioxide in dilute aquifers, *Geochem T*, *10*.

Chave, A. D., and A. G. Jones (2012), *The magnetotelluric method: Theory and practice*, Cambridge University Press.

Garcia, X., and A. G. Jones (2008), Robust processing of magnetotelluric data in the AMT dead band using the continuous wavelet transform, *Geophysics*, *73*(6), F223-F234.

García, X., and A. G. Jones (2005), A new methodology for the acquisition and processing of audio-magnetotelluric (AMT) data in the AMT dead band, *Geophysics*, *70*(5), G119-G126.

Girard, J. F., N. Coppo, J. Rohmer, B. Bourgeois, V. Naudet, and C. Schmidt-Hattenberger (2011), Time-lapse CSEM monitoring of the Ketzin (Germany) CO_2 injection using 2xMAM configuration, *10th International Conference on Greenhouse Gas Control Technologies*, *4*, 3322-3329.

Hammack, R., G. Veloski, G. Hodges, S. McLaren, and C. White (2006), An Evaluation of Helicopter and Ground Methods for Locating Existing Wells, paper presented at Symposium on the Application of Geophysics to Engineering and Environmental Problems 2006, Society of Exploration Geophysicists.

Iliceto, V., and G. Santarato (1999), On the interference of man-made EM fields in the magnetotelluric 'dead band', *Geophys Prospect*, *47*(5), 707-719.

Kelbert, A., N. Meqbel, G. D. Egbert, and K. Tandon (2014), ModEM: A modular system for inversion of electromagnetic geophysical data, *Comput Geosci-Uk*, *66*, 40-53.

Kharaka, Y. K., et al. (2010), Changes in the chemistry of shallow groundwater related to the 2008 injection of CO_2 at the ZERT field site, Bozeman, Montana, *Environ Earth Sci*, *60*(2), 273-284.

Nogues, J. P., J. M. Nordbotten, and M. A. Celia (2011), Detecting leakage of brine or CO_2 through abandoned wells in a geological sequestration operation using pressure monitoring wells, *Energy Procedia*, *4*, 3620-3627.

Ogaya Garcia, X. (2014), Magnetotelluric characterisation and monitoring of the Hontomín CO_2 storage site, Spain, University of Barcelona.

Ogaya, X., J. Ledo, P. Queralt, A. Marcuello, and A. Quinta (2013), First geoelectrical image of the subsurface of the Hontomin site (Spain) for CO_2 geological storage: A magnetotelluric 2D characterization, *Int J Greenh Gas Con*, *13*, 168-179.

Ogaya, X., P. Queralt, J. Ledo, A. Marcuello, and A. G. Jones (2014), Geoelectrical baseline model of the subsurface of the Hontomin site (Spain) for CO_2 geological storage in a deep saline aquifer: A 3D magnetotelluric characterisation, *Int J Greenh Gas Con*, *27*, 120-138.

Palacky, G. (1988), Resistivity characteristics of geologic targets, in *Electromagnetic Methods in Applied Geophysics*, edited by M. N. Nabighian, pp. 53-129, Society of Exploration Geophysicists

Reluy, F. V., J. de Paz Becares, R. Z. Hernandez, and J. S. Diaz (2004), Development of an equation to relate electrical conductivity to soil and water salinity in a Mediterranean agricultural environment, *Soil Research*, *42*(4), 381-388.

Simpson, F., and K. Bahr (2005), *Practical magnetotellurics*, Cambridge University Press.

Streich, R., M. Becken, and O. Ritter (2010), Imaging of CO_2 storage sites, geothermal reservoirs, and gas shales using controlled-source magnetotellurics: modeling studies, *Chem Erde-Geochem, 70*, 63-75.

Trainor-Guitton, W., K. Mansoor, Y. Sun, and S. Carroll (2016), Merits of pressure and geochemical data as indicators of CO_2/brine leakage into a heterogeneous, sedimentary aquifer, *Int J Greenh Gas Con*, *52*, 237-249.

Trainor-Guitton, W. J., A. Ramirez, X. J. Yang, K. Mansoor, Y. W. Sun, and S. Carroll (2013), Value of information methodology for assessing the ability of electrical resistivity to detect CO_2/brine leakage into a shallow aquifer, *Int J Greenh Gas Con*, *18*, 101-113.

Visconti, F., J. M. de Paz, and J. L. Rubio (2010), An empirical equation to calculate soil solution electrical conductivity at 25 degrees C from major ion concentrations, *Eur J Soil Sci*, *61*(6), 980-993.

Yang, X., R. N. Lassen, K. H. Jensen, and M. C. Looms (2015), Monitoring CO_2 migration in a shallow sand aquifer using 3D crosshole electrical resistivity tomography, *Int J Greenh Gas Con*, *42*, 534-544.